

OPTIMIZATION OF A DOUBLE EFFECT LiBr-H₂O ABSORPTION SYSTEM

Abebayehu Assefa
Department of Mechanical Engineering
Addis Ababa University

ABSTRACT

A computer program is developed to optimize a double-effect LiBr-H₂O absorption refrigeration system. Optimum coefficient of performance (COP) of the refrigeration system is sought for a fixed cooling load capacity of a system and fixed upper cycle pressure (pressure of *Generator 1*) and lower cycle pressure (pressure of *Evaporator/Absorber*). For any fixed upper cycle pressure and lower cycle pressure, the intermediate pressure (pressure of *Condenser/ Generator 2*) of the system is varied until the optimum COP is obtained.

The effect of increasing of the temperature of *Generator 1* on the COP of the system is also analysed. Pure water vapor is considered to be generated in both generators at the respective prevailing pressure and temperature combinations. Specific enthalpies of pure water vapor at outlet from the respective generators and the condensate water leaving the *Condenser* are automatically determined by the developed programme at the prevailing saturation temperatures. Concentrations at all state points in the cycle are also obtained from the programme at the respective state point pressure and temperature values. In the analysis, steady-state conditions and no pressure losses are assumed. The effect of the effectiveness of the heat exchangers on the COP of the system are also analysed using the developed program.

INTRODUCTION

One possible way of greatly increasing the COP of an absorption refrigeration system is incorporating a second-effect or second-stage generator. Due to its higher COP, the double-effect generation system has an improved potential for applications in absorption cooling systems than the single-effect system.

In the double-effect generation absorption cooling system, three pressure zones exist: (i) The low pressure, prevailing in the *Evaporator* and *Absorber* which is determined at the *Evaporator* temperature, (ii) The medium pressure in the *Condenser* and *Generator 2*, and (iii) The high pressure in *Generator 1* which is determined at the prevailing temperature of *Generator 2*.

In the double-effect LiBr-H₂O absorption refrigeration cycle, weak solution leaving the *Absorber* is pumped to the pressure of *Generator 1*, Fig. 1. External heat supplied to the weak solution in *Generator 1* releases water vapor from the solution. To reduce the quantity of external heat required by *Generator 1* and thus improve the performance of the system, two heat exchangers (*Heat Exchanger 1* and *Heat Exchanger 2*) are introduced as indicated. Heat transfer in *Heat Exchanger 1* to the weak solution pumped to *Generator 1* cools the strong solution entering the *Absorber*. The lower the temperature of the solution, the better the absorption rate and the lower will be the heat of absorption developed in the *Absorber*.

More refrigerant (water vapor) is vaporized in *Generator 2* by the heat of condensation of the refrigerant vapor generated in *Generator 1*. The condensate leaving the *Condenser* is throttled to the *Evaporator* pressure. After taking the cooling load in the *Evaporator*, the refrigerant vapor enters the *Absorber* to complete the cycle.

Thermal Modeling of Double Effect Generation Cycle

In the thermal modeling of the double-effect generation cycle the following assumptions are considered. The intermediate pressure of the system is in equilibrium pressure corresponding to the temperature of the *Condenser* while the low pressure and high pressure of the system correspond to the equilibrium saturation temperatures of the *Evaporator* and *Generator 1*, respectively. These assumptions along with the mass, material and energy conservations and the thermodynamic state equations lead to the complete analysis and optimization of the absorption cooling cycle.

The thermodynamic analysis of the cycle has been carried out using state equations for LiBr-H₂O system available in the literature and generated expressions. At each operating point, the LiBr-H₂O system is assumed to be in steady state at the prevailing conditions in the respective components of the cycle.

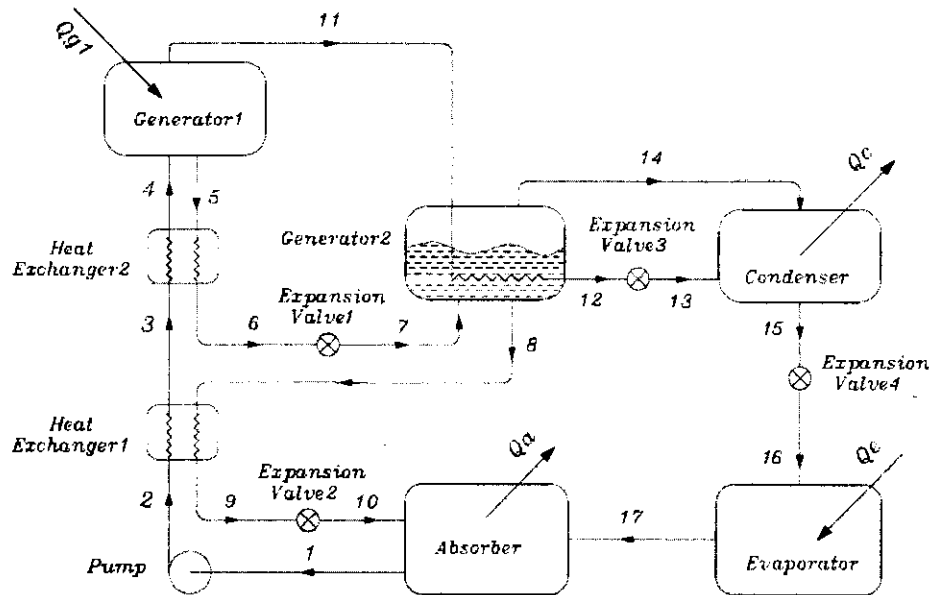


Figure 1: Double-effect generation LiBr-H₂O absorption refrigeration cycle

The analysis of the cycle is started at the **Condenser** where temperature T_C is used to determine the **Condenser** saturation pressure p_C and thus the pressure of **Generator 2**, p_{G2} . The temperature at the **Evaporator** gives the low side pressure in the **Evaporator** and the **Absorber**. From the **Absorber** temperature and the low pressure of the system, the equilibrium weak solution concentration is evaluated. The temperature in **Generator 1** and the high-pressure of the system furnish the concentration of the strong solution leaving **Generator 1**. The intermediate (medium) pressure p_{G2} and temperature T_{G2} of **Generator 2** are used to evaluate the concentration of the strong solution leaving **Generator 2**.

The acquired concentrations, pressures and temperatures at different state points, the mass, material and heat balances for each component along with the effectiveness expressions of the heat exchangers provide mass flow rates and enthalpies at each state point.

Concentrations at Various Points in the Cycle

Prevailing pressure and temperature values at each state point of the cycle are used to determine the respective concentrations. Concentration of the weak solution between state 1 to state 4 remains constant. Similarly, concentrations of the strong solution between state points 5 to state point 7 and state point 8 to state point 10 are, separately, constant. These are indicated in Eqs. (1) to (3).

Concentration of the weak solution leaving the **Absorber** is determined at the pressure p_A and temperature T_A of the **Absorber**:

$$\xi_1 = \xi(p_A, T_A) = \xi_2 = \xi_3 = \xi_4 = \xi_w \quad (1)$$

Concentration of the strong solution leaving **Generator 1** at state point 5 is obtained at p_{G1} and temperature T_{G1} of **Generator 1**.

$$\xi_5 = \xi(p_{G1}, T_{G1}) = \xi_6 = \xi_7 = \xi_{s1} \quad (2)$$

Similarly, the concentration of the stronger solution leaving **Generator 2** at state point 8 is obtained at p_{G2} and temperature T_{G2} of **Generator 2**.

$$\xi_8 = \xi(p_{G2}, T_{G2}) = \xi_9 = \xi_{10} = \xi_{s2} \quad (3)$$

where: ξ_w , ξ_{s1} and ξ_{s2} are concentrations of weak solution leaving the **Absorber**, strong solution leaving **Generator 1** and stronger solution leaving **Generator 2**, respectively.

Specific Enthalpies at the Various State Points

Specific enthalpy values at the various state points are determined as follows.

a) Saturated Liquid (Refrigerant)

The refrigerant leaving the **Condenser** at state point 15 is assumed to be saturated liquid at the **Condenser** temperature.

$$h_{15} = h_{satL} |_{T_C} = h_{16} \quad (4)$$

The vapor refrigerant leaving **Generator 1** (state 11) has to be completely condensed on leaving **Generator 2** (state 12), if the double-effect generation absorption system is to yield the maximum COP. Accordingly,

$$h_{12} = h_{satL} |_{T_{G1}} = h_{13} \quad (5)$$

b) Saturated Vapor (Refrigerant)

Refrigerants leaving the **Evaporator**, **Generator 1** and **Generator 2**, at state points 17, 11 and 14, respectively, are assumed to be saturated vapor at the temperature of the corresponding component.

$$h_{17} = h_{satV} |_{T_E}; h_{11} = h_{satV} |_{T_{G1}}; \quad (6)$$

and $h_{14} = h_{satV} |_{T_{G2}}$

c) LiBr-H₂O Solution

The specific enthalpies of the LiBr-H₂O solution at the various state points are determined at the respective prevailing temperatures and concentrations.

$$h_i = h_{sol} |_{T_A, \xi_w} = h_2 \quad (7)$$

where:

$$h_{sol} |_{T, \xi} = \sum_0^4 A_n \xi^n + T \sum_0^4 B_n \xi^n + T^2 \sum_0^4 C_n \xi^n \quad [kJ/kg] \quad (8)$$

where: T in °C and ξ in % LiBr

and

$A_0 = -2024.33$	$B_0 = 18.2829$	$C_0 = -3.7008214E-2$
$A_1 = 163.309$	$B_1 = -1.1691757$	$C_1 = 2.8877666E-3$
$A_2 = -4.88161$	$B_2 = 3.248041E-2$	$C_2 = -8.1313015E-5$
$A_3 = 6.302948E-2$	$B_3 = -4.034184E4$	$C_3 = 9.9116628E-7$
$A_4 = -2.913703E-4$	$B_4 = 1.8520569E-6$	$C_4 = -4.4441207E-9$

Concentration range: $40 < \xi < 70$ % LiBr

Temperature range: $15 < T < 165$ °C

$$h_5 = h_{sol} |_{T_{G1}, \xi_{s1}} \quad (9)$$

$$h_8 = h_{sol} |_{T_{G2}, \xi_{s2}} \quad (10)$$

$$h_9 = h_8 - \epsilon_1 (h_8 - h_{92}) = h_{10} \quad (11)$$

where: ϵ_1 = Effectiveness of **Heat Exchanger 1**

$$\epsilon_1 = \left[\frac{h_8 - h_9}{h_8 - h_{92}} \right] \quad (12)$$

and h_{92} = LiBr-H₂O solution enthalpy at concentration of state point 9 and temperature of state point 2

$$h_{92} = h_{sol} |_{T_A, \xi_{s2}} \quad (13)$$

Energy balance for **Heat Exchanger 2** yields:

$$h_3 = h_2 + \left[\frac{\dot{m}_8}{\dot{m}_2} \right] [h_8 - h_9] \quad (14)$$

$$h_6 = h_3 - \epsilon_2 (h_5 - h_{63}) = h_7 \quad (15)$$

where: ϵ_2 = Effectiveness of **Heat Exchanger 2**

$$\epsilon_2 = \left[\frac{h_5 - h_6}{h_5 - h_{63}} \right] \quad (16)$$

and h_{63} = LiBr-H₂O solution enthalpy at concentration of state point 6 and temperature of state point 3

$$h_{63} = h_{sol} |_{T_3, \xi_{s1}} \quad (17)$$

and

$$h_4 = h_3 + \left[\frac{\dot{m}_5}{\dot{m}_4} \right] [h_5 - h_6] \quad (18)$$

Mass Flow Rates

The mass flow rate of the refrigerant through the **Evaporator** can be obtained from the given load of the system and the specific enthalpy values at the **Evaporator**, as:

$$\dot{m}_r = \dot{m}_{15} = \dot{m}_{16} = \dot{m}_{17} = \frac{\dot{Q}_E}{(h_{17} - h_{16})} \quad (19)$$

Mass flow rate of weak LiBr-H₂O solution at inlet of **Generator 1** is obtained from:

$$\dot{m}_1 = \dot{m}_2 = \dot{m}_3 = \dot{m}_4 = \frac{\dot{m}_r}{\left[1 - \left\{ \frac{\xi_4}{\xi_8} \right\} \right]} = \dot{m}_w \quad (20)$$

The following relations are obtained from material balance at **Generator 1**:

$$\dot{m}_5 = \dot{m}_4 \left[\frac{\xi_4}{\xi_5} \right] = \dot{m}_6 = \dot{m}_7 \quad (21)$$

$$\dot{m}_{11} = \dot{m}_4 \left[1 - \left\{ \frac{\xi_4}{\xi_5} \right\} \right] = \dot{m}_{12} = \dot{m}_{13} \quad (22)$$

Material balance at **Generator 2** yields:

$$\dot{m}_8 = \dot{m}_5 \left[\frac{\xi_5}{\xi_8} \right] = \dot{m}_4 \left[\frac{\xi_4}{\xi_8} \right] = \dot{m}_9 = \dot{m}_{10} \quad (23)$$

Using mass and energy balances at **Generator 2**, the following relations are obtained:

$$\dot{m}_{14} = \dot{m}_4 \left[\left\{ \frac{\xi_4}{\xi_5} \right\} - \left\{ \frac{\xi_4}{\xi_8} \right\} \right] \quad (24)$$

Mass balance at the **Condenser** gives:

$$\dot{m}_{15} = \dot{m}_r = \dot{m}_4 \left[1 - \left\{ \frac{\xi_4}{\xi_8} \right\} \right] = \dot{m}_{16} = \dot{m}_{17} \quad (25)$$

Pressure-Temperature-Concentration Relations

The following expressions are applied for the determination of the pressure, temperature and concentration of LiBr-H₂O solution:

$$\left. \begin{aligned} t &= \sum_0^3 B_n \xi^n + t' \sum_0^3 A_n \xi^n; \text{ Solution temperature } [^{\circ}\text{C}] \\ t' &= \frac{\left(t - \sum_0^3 B_n \xi^n \right)}{\sum_0^3 A_n \xi^n}; \text{ Refrigerant temperature } [^{\circ}\text{C}] \\ \log P &= C + D/T' + E/T'^2; \text{ Pin [kPa] and T' in [K]} \\ T' &= \frac{-2E}{D + \left\{ D^2 - 4E(C - \log P) \right\}^{0.5}} \end{aligned} \right\} \quad (26)$$

where:

$$\left\{ \begin{array}{lll} A_0 = -2.00755 & B_0 = 124.937 & C = 7.05 \\ A_1 = 0.16976 & B_1 = -7.71649 & D = -1596.49 \\ A_2 = -3.133362E-3 & B_2 = 0.152286 & E = -104095.5 \\ A_3 = 1.97668E-5 & B_3 = -7.95090E-4 & \end{array} \right.$$

where:

$$\begin{aligned} \text{Concentration range: } & 45 < \xi < 70 \% \text{ LiBr} \\ \text{Temperature range: } & 5 < t < 175^{\circ}\text{C} \\ & -15 < t' < 110^{\circ}\text{C} \end{aligned}$$

The concentration at any particular state point with specified pressure and temperature is determined through a process of iteration. The iteration procedure is exemplified considering the determination of the concentration of the weak-solution leaving the **Absorber**. At the **Absorber** pressure p_A , which is held constant during the iteration process, and solution temperature T_A , an initial concentration value ξ_w within the range ($45 < \xi < 70 \% \text{ LiBr}$) is assumed. For a fixed pressure p_A and the assumed solution concentration ξ_w , t' in $^{\circ}\text{C}$ and solution temperature t are determined from Eq.(26). The calculated solution temperature t is then compared with the actual solution temperature T_A . If $|T_A - t|$ is not less than 0.0001 (set error limit), then the assumed concentration is adjusted by ± 0.0001 and a mean value of the previous concentration and the new value of concentration is applied to calculate a new value of t from Eq. (26). The process of adjusting the concentration and determination of the solution temperature t from Eq.(26) is repeated until the difference between the actual solution temperature T_A and the calculated solution temperature t is within the set error limit. The concentration value thus obtained is the concentration of the solution at pressure p_A and solution temperature T_A . This procedure is also applied in the determination of the strong-solution concentrations ξ_{S1} and ξ_{S2} at outlet from **Generator 1** and **Generator 2**, respectively, Fig. 3.

Heat Transfer Duties and COP of the System

The heat transfer duties of the various components of the double-effect LiBr-H₂O system are determined from application of energy balance.

a) Absorber:

The heat of absorption in the **Absorber** is given by:

$$\begin{aligned} \dot{Q}_A &= \dot{m}_8 h_{10} + \dot{m}_{15} h_{15} - \dot{m}_1 h_1 \\ &= \dot{m}_4 \left[\frac{x_2}{x_8} \right] h_9 + \dot{m}_{15} h_{15} - \dot{m}_1 h_1 \end{aligned} \quad (27)$$

b) Generator 1:

Energy balance at **Generator 1** gives:

$$\dot{Q}_{G1} = \dot{m}_5 h_5 + \dot{m}_{11} h_{11} - \dot{m}_4 h_4 \quad (28)$$

c) Generator 2:

The quantity of heat released by the vapor leaving **Generator 1** and absorbed by solution in **Generator 2** is given by:

$$\dot{Q}_{G2} = \dot{m}_{11} (h_{11} - h_{12}) \quad (29)$$

d) **Condenser:**

Energy balance at the **Condenser** gives:

$$\dot{Q}_C = \dot{m}_{13} h_{13} + \dot{m}_{14} h_{14} - \dot{m}_{15} h_{15} \quad (30)$$

The **coefficient of performance (COP)** of the double effect absorption cycle is given by:

$$COP = \frac{Q_E}{Q_{G1}} \quad (31)$$

A double-effect generation LiBr-H₂O absorption refrigeration cycle is represented on a **P-T-ξ** in Fig.2. The numbers on this figure correspond to the state points indicated on the double-effect absorption cycle, Fig. 1.

System Optimization Flow Chart

A flow-chart illustrating the optimization process of the double-effect LiBr-H₂O absorption refrigeration

model is given in Fig. 3.

Discussion of Results

The LiBr-H₂O absorption refrigeration cycle model is analyzed based on values chosen from the actual ranges over which the machine is expected to operate. Accordingly, the following data are considered for the analysis.

$$\begin{aligned} \dot{Q}_E &= 10 \text{ kW}; p_E = p_A = 2.0 \text{ kPa}; \\ p_C = p_{G2} &= 5 \text{ kPa}; p_{G1} = 15 \text{ kPa}; \\ \epsilon_1 = \epsilon_2 &= 90\%; \xi_w = 45\%; \xi_{S1} = 50\%; \\ \xi_{S2} &= 55\%. \end{aligned}$$

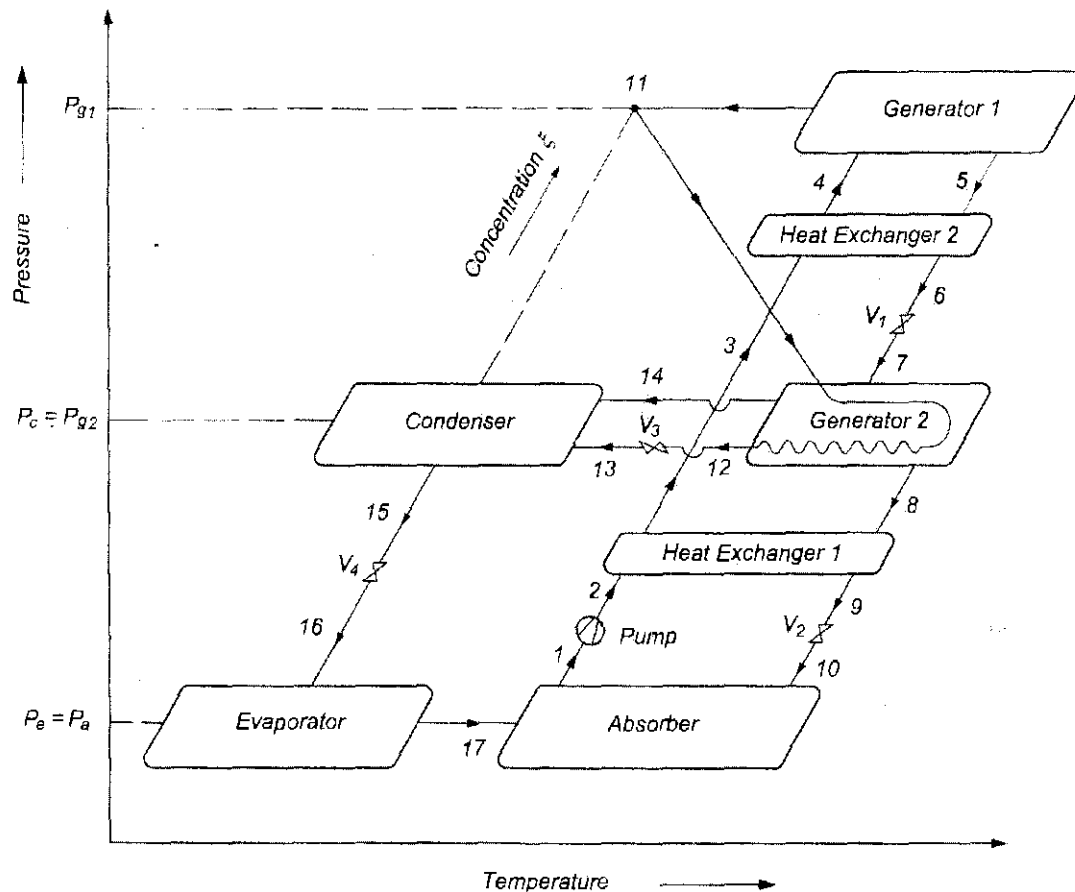


Figure 2 P-T-ξ Representation of Double-Effect Generation LiBr-H₂O Absorption Refrigeration Cycle

Using the steady state equations for the thermodynamic properties of LiBr-H₂O, the effects

varying parameters on the coefficient of performance (COP) of the system were analysed. The maximum COP of the double effect absorption refrigeration system of the example considered (1.855) is about twice that of the COP of a single effect absorption refrigeration system (0.901). The effect of increasing the temperature of *Generator 2* and thus its pressure and the pressure of the condenser, keeping the concentration of the strong

solution leaving it constant at $\xi_{s2} = 55\%$, increases the COP of the system until the heat of condensation of the refrigerant vapor generated in *Generator 1* is equal to the energy absorbed by the solution in *Generator 2*, Fig. 4. The COP of the double-effect absorption refrigeration is optimum, for the specified fixed upper cycle pressure (pressure of *Generator 1*) and lower cycle pressure (pressure of *Evaporator/Absorber*), at about $T_{G2} = 60.5^\circ\text{C}$.

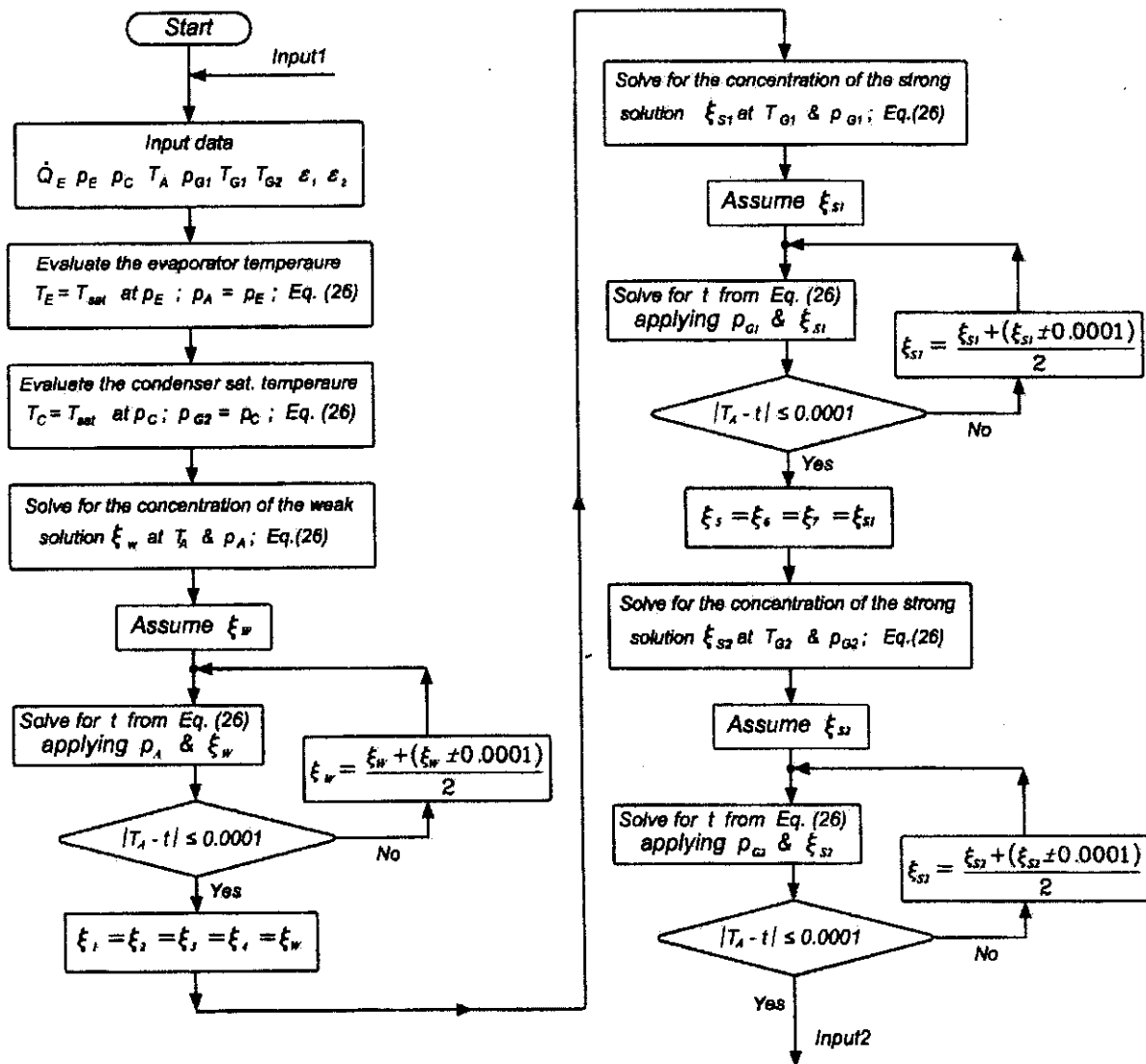


Figure 3 Flow Chart for Computer Simulation of the Double-Effect Generation LiBr-H₂O Absorption Refrigeration Cycle

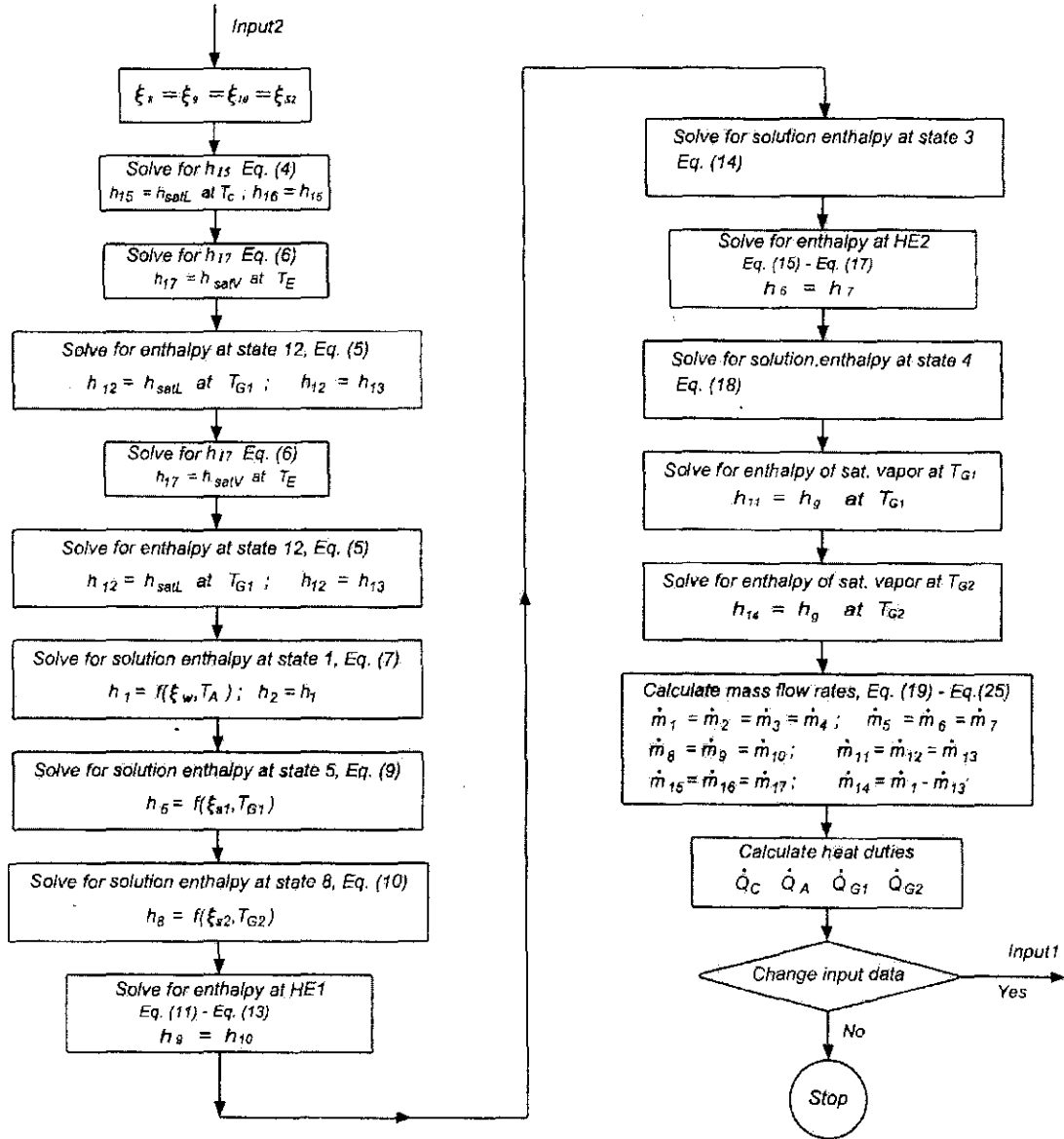


Figure 3 Flow Chart for Computer Simulation of the Double-Effect Generation LiBr-H₂O Absorption Refrigeration Cycle (Continued)

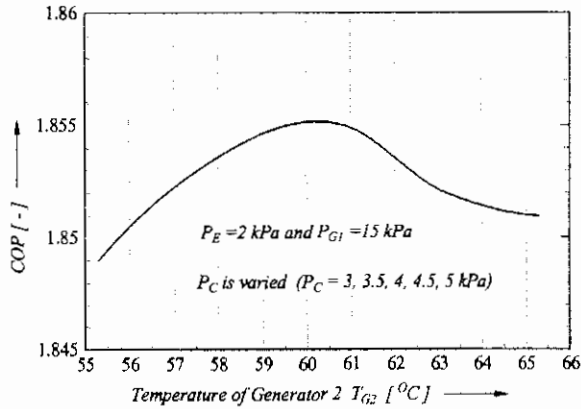


Figure 4 Effect of Temperature of Generator 2 on COP of the System

The effect of increasing the temperature of **Generator 1** on the COP of the system, for fixed evaporator and condenser pressures, is shown in Fig.5. Increasing the temperature of **Generator 1** increases the generator capacity. And as may be expected (Eq. (31)), for a fixed cooling load, increasing the generator capacity reduces the COP of the system. The effect of increasing the temperature of **Generator 1** is performed for two cases. In the first case, the temperature of **Generator 1** and its corresponding pressure are varied while the concentration of the solution leaving **Generator 1** is maintained constant. In the second case, the pressure of **Generator 1** is maintained constant and the temperature of **Generator 1** and concentration of the solution leaving **Generator 1** are varied. The latter case shows a drastic drop in the COP of the system while the drop in COP is insignificant for the first case, Fig. 5.

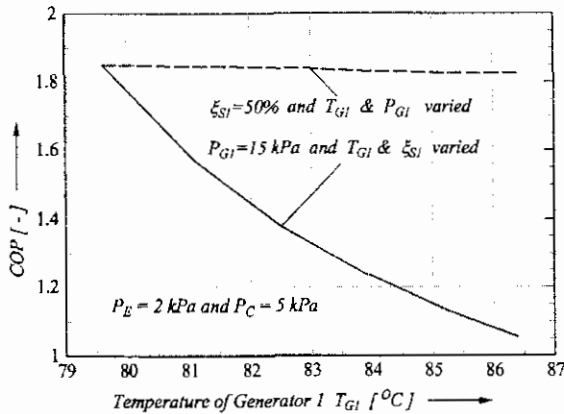


Figure 5 Effect of Temperature of Generator 1 on COP of the System

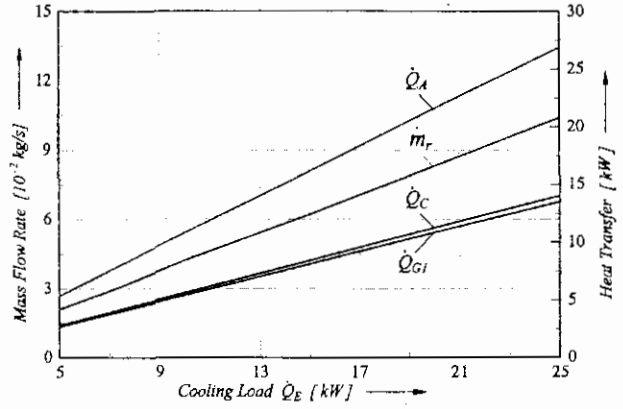


Figure 6 Effect of Varying Cooling Load Q_E on Mass Flow Rate and Heat Transfer Rates

The effect of varying the cooling load on the mass flow rate of the refrigerant and the heat transfer loads in the various components is shown in Fig. 6. As cooling load in the evaporator increases, the mass flow rate of the refrigerant in the system increases. The rate of heat transfer in the various components thus increases proportional to the increase in the refrigerant mass flow rate.

A decrease in the COP of the system is observed with increasing values of **Evaporator** pressure p_E , for fixed pressures of **Condenser and Generator 1**, Fig. 7.

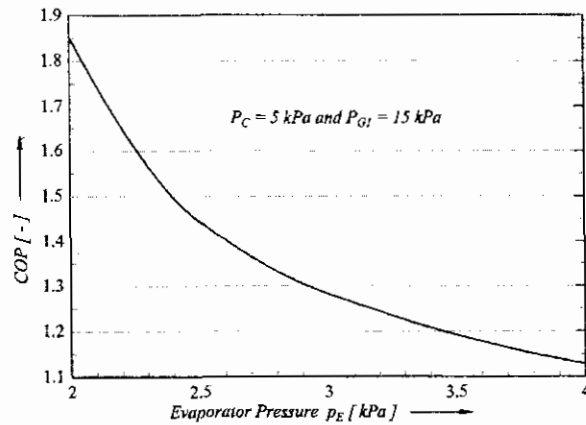


Figure 7 Effect of Varying Evaporator Pressure p_E

The effect of solution heat exchangers effectiveness is depicted in Fig. 8. The effectiveness of heat exchangers markedly affect the COP of the system. Keeping all other parameters fixed and varying the effectiveness of **Heat Exchanger 1** from the original value of $\epsilon_1 = 90\%$ to $\epsilon_1 = 65\%$ reduces the COP of the system from 1.851 to 1.825. The effect of **Heat**

Exchanger 2 on the COP of the system is more pronounced as its value reduces from 1.851 to 1.755 for the same range of effectiveness drop, $\epsilon_2 = 90\%$ to $\epsilon_2 = 65\%$. The reduction in the COP of the system would even be lower if the effectiveness of both heat exchangers is simultaneously reduced from $\epsilon_{12} = 90\%$ to $\epsilon_{12} = 65\%$.

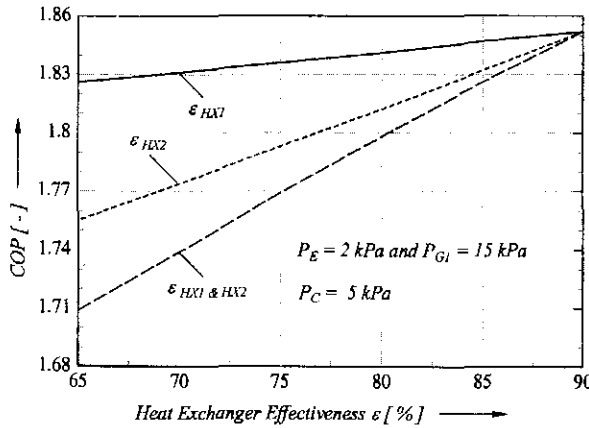


Figure 8 Effect of Heat Exchanger Effectiveness on COP of the System

NOMENCLATURE

- COP = Coefficient of performance of double-effect absorption refrigeration system [-]
- h = Specific enthalpy [kJ/kg]
- \dot{m} = Mass flow rate [kg/s],
- p_A = Absorber pressure [kPa]
- p_C = Condenser pressure [kPa]
- p_E = Evaporator pressure [kPa]
- p_{G1} = Generator 1 pressure [kPa]
- p_{G2} = Generator 2 pressure [kPa]
- \dot{Q}_c = Heat rejected in the Condenser [kW],
- \dot{Q}_E = Heat absorbed by refrigerant in the Evaporator (Cooling load of the system) [kW],
- \dot{Q}_A = Heat of absorption in the Absorber [kW],
- \dot{Q}_{G1} = Heat received by weak solution in Generator 1 [kW],
- \dot{Q}_{G2} = Heat released by water vapor in Generator 2 [kW],

- T_A = Absorber temperature [$^{\circ}$ C]
- T_C = Condenser temperature [$^{\circ}$ C]
- T_E = Evaporator temperature [$^{\circ}$ C]
- T_{G1} = Generator 1 temperature [$^{\circ}$ C]
- T_{G2} = Generator 2 temperature [$^{\circ}$ C]
- ξ = Concentration of LiBr-H₂O solution [%]
- ξ_{S1} = Concentration of solution leaving Generator 1 [%]
- ξ_{S2} = Concentration of solution leaving Generator 2 [%]
- ξ_W = Concentration of weak solution leaving Absorber [%]
- ϵ_1, ϵ_2 = Effectiveness of Heat Exchanger 1 and Heat Exchanger 2, respectively [-]

REFERENCES

- [1] Xu, G. P., Dai, Y. Q., Tou, K. W. and Tso, C. P., Theoretical Analysis and Optimization of a Double-Effect Series-Flow-Type Absorption Chiller, Applied Thermal Engineering, Volume 16, Issue 12, December 1996, Pages 975-987.
- [2] Wardono B., Nelson R., Simulation of a Double-Effect LiBr/H₂O Absorption Cooling System, Fuel and Energy Abstracts, Vol. 38, Number 4, July 1997, pp. 262-262(1), Elsevier.
- [3] Atsushi, A., Improvement of the COP of the LiBr-Water Double-Effect Absorption Cycles, Transactions of the Japan Society of Refrigerating and Air Conditioning Engineers, Vol. 17, No.3, Page 257-268, 2000.
- [4] Liu, Y. L. and Wang, R. Z., Performance Prediction of a Solar/Gas Driving Double Effect LiBr-H₂O Absorption System, Renewable Energy Journal, Vol. 29, No.10, pp. 1677-1695, 2004.
- [5] ASHARE Handbook of Fundamentals, New York: American Society of Heating, Refrigerating and Air Conditioning Engineers, Inc., pp. 16.79-16.82, 1977.

- [6] ASHRAE Guide Data Book, Equipment & Systems 2000, American Society of Heating, Refrigeration and Air Conditioning Engineers, New York, 2000.
- [7] Ballaney, P.L., Refrigeration and Air Conditioning, Khanan Publishers, 13th Edition, 2002.
- [8] Herold, K.E., Radermacher, R. and Klein, S.A., Absorption Chillers and Heat Pumps, CRC Press, Inc., 1996.
- [9] Herold, K.E. and Moran, M.J., Thermodynamic Properties of Lithium Bromide/Water Solutions, ASHRAE Transactions, Vol. 85, Part 2, pp. 413-434, 1979.
- [10] Holman, J.P., Heat Transfer, McGraw-Hill, Inc., New York, 1996.
- [11] Kaushik, S.C., Advanced Solar Absorption Refrigeration and Air Conditioning System, IIT Delhi, India, 1986.
- [12] Lee, S.F. and Sherif, S.A., Thermodynamic Analysis of a Lithium Bromide/Water Absorption System for Cooling and Heating Applications, Int. Journal of Energy Research, Vol. 25, pp. 1019-1031, 2001.
- [13] McNeely, L.A., Thermodynamic Properties of Aqueous Solutions of Lithium Bromide, ASHRAE Transactions, Vol. 93, Part 1, pp. 35-50, 1987.
- [14] Shah, R.K. and Sekulić, D.P., Fundamentals of Heat Exchanger Design, John Wiley & Sons, Inc. New Jersey, 2003.
- [15] Warren, M.R., Jamesp, H. and Young, I.C., Hand Book of Heat Transfer, 3rd Edition, McGraw-Hill, New York, 1998.